Med Ultrason 2025, Vol. 27, no. 4, 497-508

Early detection of recurrent cellulitis over an erythematous scar by high-frequency ultrasound

Ya-Ling Huang, Chia-Yu Kuo

Department of Physical Medicine and Rehabilitation, Cathay General Hospital, Taipei City, Taiwan

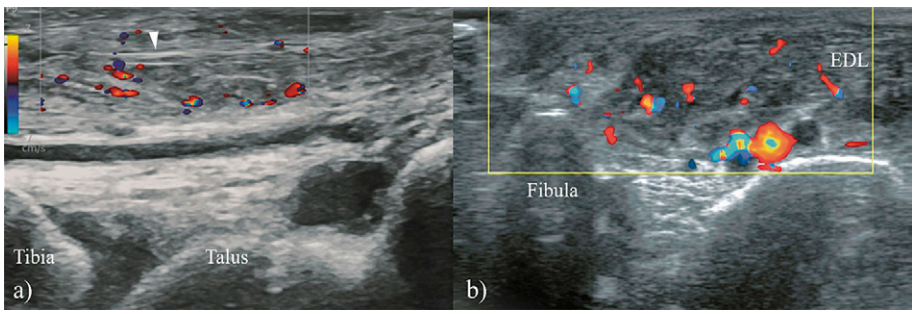

Fig 1. a) Ultrasound image at noon demonstrating hypoechoic swelling and markedly increased vascularity within the soft tissues surrounding the extensor digitorum longus (EDL) tendon (white arrowhead). b) The follow-up ultrasound image at 9 pm revealed intensified Doppler signals extending proximally along the EDL muscle.

To the Editor,

A 33-year-old female presented with classical cellulitis symptoms of pain, redness, and warmth over an erythematous hypertrophic scar on her ankle from a traffic accident three years prior. The scar was located over the extensor digitorum longus (EDL) tendon. Oral antibiotics (Augmentin) were prescribed and the infection subsided.

Two days after completing one course of antibiotics, the patient experienced recurrent mild redness at noon, though without severe pain, warmth, or swelling typically associated with cellulitis. High-frequency ultrasound demonstrated markedly increased vascularity and hypoechoic swelling within the soft tissue near the EDL tendon (fig 1a), preceding the progression of external signs. The dermatologist initially favored a localized inflammatory process over an infection. However, within nine hours, the erythema spread, and the patient's pain became apparent. The repeated ultrasound showed increased Doppler signals extending proximally along the EDL muscle (fig 1b). Prompt re-initiation of antibiotic therapy halted the progression with rapid clinical improvement.

Ultrasound is valuable for the early detection of cellulitis, particularly when clinical findings are equivocal. In this case, sonographic hyperemia and subtle swelling revealed the evolving infection before overt clinical manifestations. While most studies emphasize the classic "cobblestone" sign of soft tissue infection, the early changes seen here, including increased vascularity and rapid adjacent spread, are also highly informative [1].

In conclusion, high-frequency ultrasound is an essential tool for early detection and real-time monitoring of skin and soft tissue infections. It enables the visualization of subtle pathological changes, including hypervascularity and spread into surrounding tissues, before classical clinical signs emerge. This ensures timely intervention and effective patient management.

Received 11.09.2025 Accepted 08.11.2025
Med Ultrason
2025, Vol. 27, No 4, 497, DOI: 10.11152/mu-4562,
Corresponding author: Chia-Yu Kuo
280, Sec. 4, Ren'ai Rd.,
Da'an Dist., Taipei City 106,
Taiwan
Phone 886-2-2708-2121
E-mail: cgh22000@cgh.org.tw

Reference

1. Marks A, Schraft E, Gottlieb M. Skin, soft tissue, and musculoskeletal ultrasound. Emerg Med Clin North Am 2024;42:863-890.

A dynamic ultrasound-based framework for diagnosing subacromial impingement and predicting response to guided injection: the CHANG protocol

Ke-Vin Chang[1,2,3], Wei-Ting Wu[1,2], Levent Özçakar[4]

[1]Department of Physical Medicine and Rehabilitation and Community and Geriatric Research Center, National Taiwan University Hospital, Bei-Hu Branch, [2]Department of Physical Medicine and Rehabilitation, National Taiwan University College of Medicine, Taipei, Taiwan, [3]Center for Regional Anesthesia and Pain Medicine, Wang-Fang Hospital, Taipei Medical University, Taipei, Taiwan, [4]Department of Physical and Rehabilitation Medicine, Hacettepe University Medical School, Ankara, Turkey

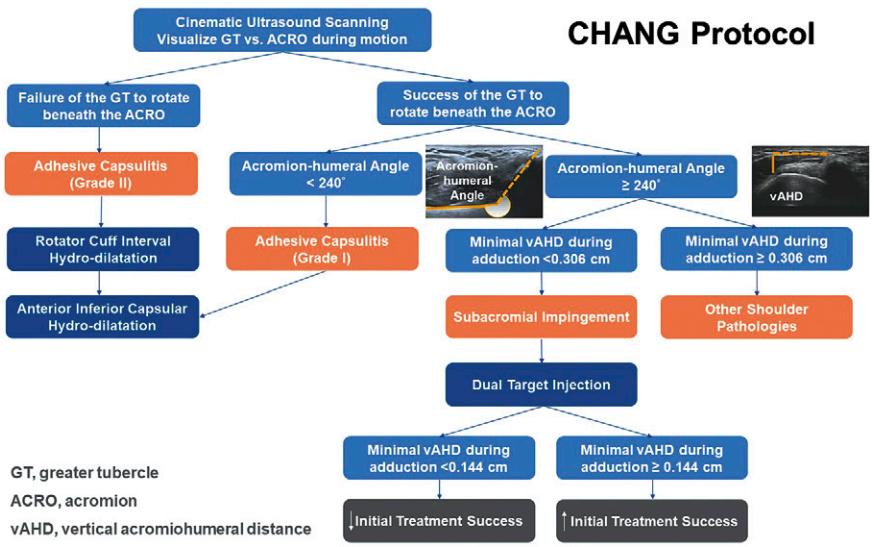

Fig 1. Flow diagram of the CHANG protocol.

To the Editor,

The CHANG Protocol – an acronym for Cinematic ultrasound tracking, Humeral-Acromial kinematics, Assessment of mechanical impingement, Needle-Guided intervention and outcome prediction – is a structured, ultrasound-based framework designed for the diagnosis and management of shoulder disorders through dynamic evaluation and targeted treatment (fig 1). The protocol begins with cinematic ultrasound tracking, which captures real-time motion of the greater tubercle relative to the acromion during shoulder abduction and enables visualization of dynamic impingement. This is followed by the analysis of humeral-acromial kinematics, where the vertical acromiohumeral distance (vAHD), is quantitatively assessed throughout the motion arc.

This dynamic assessment facilitates the identification of mechanical impingement and, once abnormalities are detected, ultrasound guided injection. Subsequently, outcome prediction is applied to distinguish between adhesive capsulitis and subacromial impingement via a stepwise diagnostic algorithm. With the transducer placed laterally over the scapular plane, the patient per-

Received 12.05.2025 Accepted 21.07.2025
Med Ultrason
2025, Vol. 27, No 4, 498-499, DOI: 10.11152/mu-4563,
Corresponding author: Ke-Vin Chang, MD, PhD
Department of Physical Medicine and Rehabilitation, National Taiwan University Hospital, Bei-Hu Branch and National Taiwan University College of Medicine,
Taipei, Taiwan
E-mail: kvchang011@gmail.com

forms shoulder abduction. Lack of rotation of the greater tubercle beneath the acromion confirms adhesive capsulitis (Grade 2). If rotation is preserved but the acromion-humeral angle remains below 240°, a milder presentation (Grade 1) is diagnosed [1].

Treatment is stratified according to severity. Patients with Grade 1 adhesive capsulitis undergo immediate anterior-inferior glenohumeral capsular distension [2]. In contrast, those with Grade 2 first receive hydro-dilatation of the rotator cuff interval [3], followed by reassessment. Capsular intervention is recommended once the condition has improved to Grade 1. This delay in capsular intervention for Grade 2 cases is necessary due to the increased resistance from severe adhesions. If the rotator interval is not addressed beforehand, direct capsular injection may encounter excessive resistance, which can place significant strain on the injector's wrist.

Subacromial impingement is suspected when the acromion-humeral angle exceeds 240°. In such cases, a dynamic "raise-and-drop" maneuver is performed for three cycles. A minimal vAHD of less than 0.306 cm during adduction confirms the diagnosis. If the minimal vAHD is ≥0.306 cm [4], alternative diagnoses should be considered. These patients are treated with dual-target injections involving both the biceps long head tendon sheath and subdeltoid bursa. Additionally, a minimal vAHD of less than 0.144 cm is predictive of a higher risk of initial treatment failure [5].

In summary, the CHANG Protocol offers a motion-based diagnostic and therapeutic framework for shoulder disorders. Integration with artificial intelligence enables automated analysis of subacromial motion, improving diagnostic precision and scalability. Large artificial intelligence-derived ultrasound datasets help refine cut-off values, enhancing predictive accuracy.

Acknowledgment: The present study was funded by National Taiwan University Hospital, Bei-Hu Branch (grant nos. 113-BH002 and 113-BH004), the Ministry of Science and Technology (grant nos. MOST 106-2314-B-002-180-MY3, 109-2314-B-002-114-MY3, 111-2314-B-002–161, NSTC 113-2314-B-002-208-MY2 and NSTC 113-2314-B-002-209-MY2), and Taiwan Society of Ultrasound in Medicine.

References

1. Chang KV, Wu WT, Shu YC, Lin CY, Özçakar L. Humerus-acromion angle model: a novel dynamic ultrasound technique for assessing shoulder mobility in adhesive capsulitis. Med Ultrason 2025;27:246-247.
2. Chang KV, Wu WT, Özçakar L. A Novel Sonographic Approach for Immediate Mobility Restoration in Adhesive Capsulitis: Anterior-Inferior Glenohumeral Joint Hydro-Dilatation. Am J Phys Med Rehabil 2025;104:1038-1039.
3. Wang JC, Tsai PY, Hsu PC, et al. Ultrasound-Guided Hydrodilatation With Triamcinolone Acetonide for Adhesive Capsulitis: A Randomized Controlled Trial Comparing the Posterior Glenohumeral Recess and the Rotator Cuff Interval Approaches. Front Pharmacol 2021;12:686139.
4. Wu WT, Lin CY, Shu YC, Chen LR, Özçakar L, Chang KV. Subacromial Motion Metrics in Painful Shoulder Impingement: A Dynamic Quantitative Ultrasonography Analysis. Arch Phys Med Rehabil 2023;104:260-269.
5. Wu WT, Lin CY, Shu YC, Chen LR, Özçakar L, Chang KV. Predictive value of subacromial motion metrics for the effectiveness of ultrasound-guided dual-target injection: a longitudinal follow-up cohort trial. Insights Imaging 2025;16:145.

Uterine rupture during the second trimester

Zhengfeng Zhu, He-Zhou Li

Ultrasound department, Zhengzhou University Third Hospital and Henan Province Women and Children's Hospital, Zhengzhou, China

Received 30.08.2025 Accepted 13.09.2025
Med Ultrason
2025, Vol. 27, No 4, 499-500, DOI: 10.11152/mu-4564,
Corresponding author: He-Zhou Li
ZhengZhou University Third Hospital and Henan Province Women and Children's Hospital, Zhengzhou, China
E-mail lihezhou67@126.com

To the Editor,

Uterine rupture constitutes a considerable risk factor contributing to maternal and fetal morbidity and mortality, especially in patients with prior cesarean deliveries. Enhancing diagnostic protocols is crucial for improving patient outcomes.

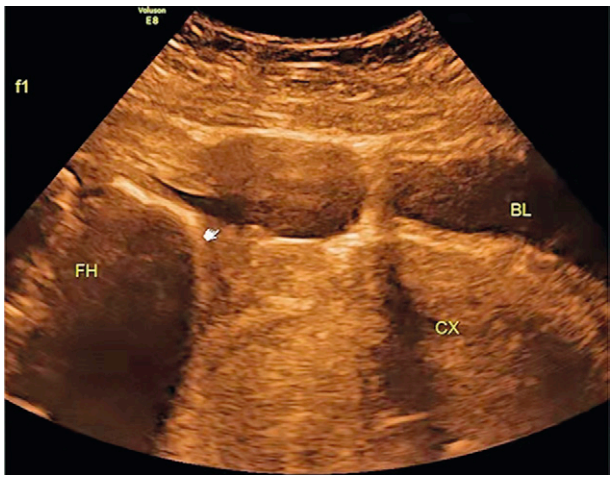

Fig 1. Preoperative ultrasound demonstrating a markedly interrupted myometrium and a bulging sac with thin membrane, suggesting uterine dehiscence.

A 35-year-old G3P2 chorionic twin pregnancy underwent routine transabdominal ultrasound at 23 weeks. She had two prior cesarean deliveries. The continuity of the myometrium in the lower segment of the uterus was interrupted and uterine dehiscence was suspected as it seemed that serosal layer was intact, with anechoic areas protruding (fig 1) [1]. Intraoperative diagnosis was uterine rupture. The bulging was the amniotic sac.

Uterine rupture is a complete division of all three layers (endometrium, myometrium, and perimetrium) of the uterus; uterine dehiscence is a partial division. Uterine rupture cases could present typical signs like abdominal pain, abdominal tenderness, vaginal bleeding, hemoperitoneum, and hemodynamic instability. It should be noted that it may also be asymptomatic [2]. Mid-gestational uterine rupture is rare, and the lack of symptomatic manifestation could make their evaluation and management more challenging. Maternal outcomes are also worse compared with those late-pregnancy rupture.

In patients with previous uterine scars, second-trimester routine ultrasonography should focus on the continuity of the lower uterine anterior wall. Uterine dehiscence demonstrated a thin uterine wall segment and bulging at the old cesarean scar segment [1,3]. A protruding amniotic sac from a completely ruptured uterus may have similar ultrasound findings. The amniotic membrane of protruding amniotic sac may be misdiagnosed as the serosal layer under ultrasound. This requires paying attention to more relevant ultrasonographic imaging features to assist in the identification for the risk of uterine rupture, even if no symptoms were present in pregnant women with prior cesarean.

References

1. Zhu Z, Li H, Zhang J. Uterine dehiscence in pregnant with previous caesarean delivery. Ann Med 2021;53:1265-1269.
2. Sun SV, Young K, Fry RC, Manuck TA. Sonographic and genetic findings in a case of asymptomatic spontaneous uterine rupture. Ultrasound Obstet Gynecol 2022;59:398-399.
3. Sarue P, Eynon N, Zbeidy RA. Uterine Dehiscence: A Diagnostic Conundrum in Repeat Cesarean Deliveries. Clin Case Rep 2025;13:e70791.

Masson's tumor mimicking venous thrombosis: a cephalic vein case

Chengmei He, Zhitong Ge, Zhonghui Xu, Jianchu Li

Department of Ultrasound, State Key Laboratory of Complex Severe and Rare Diseases, Peking Union Medical College Hospital, Chinese Academy of Medical Science & Peking Union Medical College, Beijing China

Received 27.08.2025 Accepted 13.09.2025
Med Ultrason
2025, Vol. 27, No 4, 500-501, DOI: 10.11152/mu-4565,
Corresponding author: Jianchu Li
Department of Ultrasound, State Key Laboratory of Complex Severe and Rare Diseases, Peking Union Medical College Hospital, Chinese Academy of Medical Science & Peking Union Medical College, Beijing 100730, China
E-mail: jianchuli_0301@163.com

To the Editor,

A 38-year-old woman presented with a 2-week history of a firm, mobile subcutaneous nodule on her right radial wrist following heavy lifting. Initial ultrasound at another institution identified a 1.2×0.3 cm hypoechoic lesion within the cephalic vein that was misdiagnosed as thrombus, leading to unsuccessful anticoagulation therapy. Upon referral to our institution, repeat ultrasound

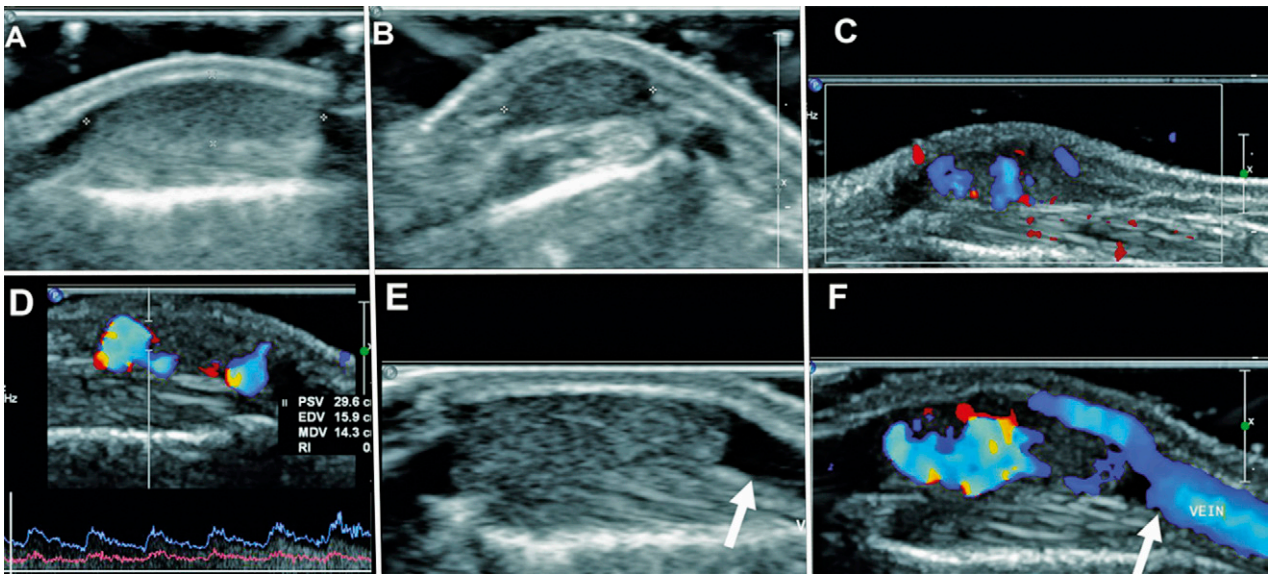

Fig 1. A) Longitudinal grayscale US shows a well-defined, heterogeneously hypoechoic oval mass; B) transverse view of the mass; C) Color Doppler reveals rich vascularity with linear signals; D) Spectral Doppler demonstrates arterial flow; E) Grayscale US shows adjacent cephalic vein dilatation; F) Color Doppler confirms vascularity within the dilated vein.

demonstrated a well-defined, hypoechoic mass (fig 1A-B) (1.2×0.7×0.4 cm) in the cephalic vein with internal linear vascular signals (fig 1C) and arterial spectrum on Doppler (fig 1D), raising suspicion for Masson's tumor (intravascular papillary endothelial hyperplasia, IPEH). The affected cephalic vein appeared markedly dilated (fig 1E-F). Surgical excision confirmed the diagnosis histopathologically, demonstrating papillary endothelial proliferation with fibrin deposition and positive vascular markers (SMA, CD31/CD34). Follow-up at one year showed no evidence of recurrence.

IPEH is a benign vascular tumor that was first described by Pierre Masson in 1923. IPEH typically develops within thrombosed blood vessels or pre-existing vascular malformations. Histopathologically, IPEH features intravascular papillary structures lined by hyperplastic yet cytologically bland endothelial cells [1]. Clinically, most lesions present as 1-2 cm painless, slowly enlarging subcutaneous nodules, with predilection for the head, neck, fingers, and trunk. IPEH has three subtypes: primary (dilated vessels), secondary (vascular malformations), and extravascular (hematomas). The present case, involving the cephalic vein of the wrist, corresponds to the primary form. Complete surgical excision is the gold standard treatment, with recurrence rates <10% after complete resection.

Definitive IPEH diagnosis relies on histopathology due to nonspecific imaging features. For superficial lesions, ultrasonography is the primary imaging modality, especially when masses are too small for CT or MRI. Color Doppler offers valuable supplemental information on vascular patterns. On ultrasound, IPEH often appears as hypoechoic intravascular lesion with internal vascularity on Doppler, in contrast to non-vascularized thrombus. Kim et al. analyzed ultrasound characteristics of ten subcutaneous IPEH cases, consistently observing well-defined margins and hypoechoic features [2]. Heterogeneous lesions contained more varied stage organizing thrombi with prominent fibrous septa compared to homogeneous ones. Pathologically, these internal septations correspond to fibrin-rich connective tissue within organizing thrombi. Subcutaneous IPEH also needs to be differentiated from other conditions: vascular angioleiomyoma, circumferential hemangioma, non-subungual glomus tumor, neurogenic tumor, and other soft tissue masses. While ultrasound alone cannot definitively diagnose IPEH, it plays a critical role in prompting further investigation when atypical features are observed.

Acknowledgment: This work was supported by National High Level Hospital Clinical Research Funding (2022-PUMCH-B-064).

References

1. Yang K, Pan CX, Russell-Goldman EE, Nambudiri VE. Characterization of intravascular papillary endothelial hyperplasia: a multicentre cohort. Clin Exp Dermatol 2022; 47:1550-1553.
2. Kim OH, Kim YM, Choo HJ, et al. Subcutaneous intravascular papillary endothelial hyperplasia: ultrasound features and pathological correlation. Skeletal Radiol 2016;45: 227-233.

One case of intraocular non-neoplastic space-occupying lesion diagnosed by contrast-enhanced ultrasound

Min Qiao*, Jiamei Ji*, Dejuan Shen, Xiaoqin Qian

** the authors share the first authorship*

Department of Ultrasound, Northern Jiangsu People's Hospital, Yangzhou, Jiangsu, China

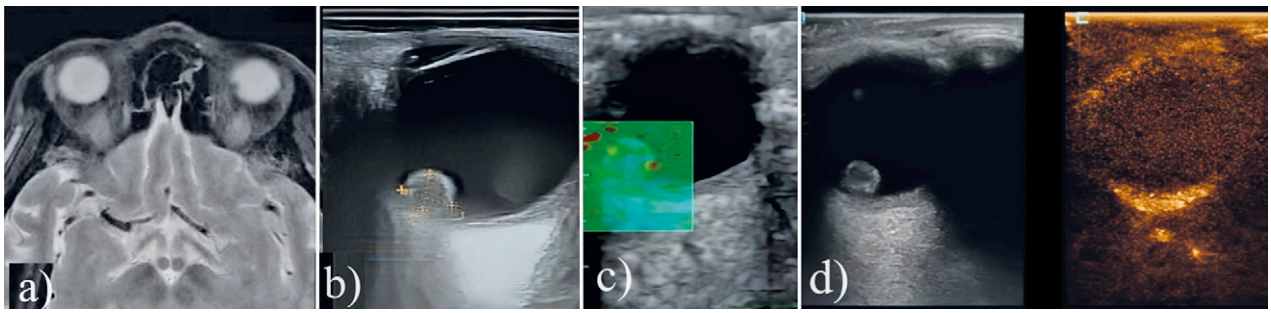

Fig 1. a) MRI revealed a nodule located on the posterior inner wall of the left eyeball; b) Ultrasound demonstrated a hemispherical hypoechoic lesion on the nasal side of the left optic disc, measuring approximately 5.4×4.5×3.6 mm; c) Ultrasound elastography indicated a moderate elasticity; d) Contrast-enhanced ultrasound showed no enhancement in the lesion area.

To the Editor,

A 66-year-old male patient presented to our hospital with the chief complaint of "suddenly declined vision of left eye for two days". The patient denied a history of diabetes or trauma. Fundoscopy revealed bloody opacity of the vitreous body and indistinct retina. MRI revealed a nodule located on the posterior inner wall of the left eyeball, suggestive of a space-occupying lesion requiring further exclusion (fig 1a). Ultrasound examination demonstrated dense punctate echoes and movable continuous band-like hyperechoic regions within the vitreous body of the left eye, which were connected to the posterior pole of the globe with no blood flow signals. A hemispherical hypoechoic lesion was identified on the nasal side of the left optic disc, measuring approximately 5.4×4.5×3.6 mm, with uncertain blood flow signals (fig 1b). Ultrasound elastography indicated a moderate elasticity (fig 1c). The conclusion was vitreous opacity, posterior vitreous detachment of the left eye with the possibility of an intraocular space-occupying lesion. To further clarify the diagnosis, contrast-enhanced ultrasound was performed, which showed no enhancement in the lesion area, raising the possibility of vitreous hemorrhage (fig 1d). The patient was admitted for surgical exploration. In the operation, vitreous hemorrhage was observed, and a large oval-shaped blood clot was found anterior to the retina, which was removed subsequently.

Vitreous hemorrhage (VH) refers to bleeding that occurs within the vitreous cavity of the eye. It typically presents symptoms such as decreased visual acuity, dark shadows in the visual field, and perception of floaters. Common causes include ocular trauma, proliferative diabetic retinopathy, and posterior vitreous detachment with or without retinal tear [1,2]. This case is considered to be caused by posterior vitreous detachment. VH can rapidly form blood clots. Because vitreous gel is rich in collagen, it can promote platelet aggregation and the blood clot formation [2]. Newly formed blood clots may present as hypoechoic on ultrasound imaging and gradually transform into isoechoic or mixed echogenicity. In color Doppler flow imaging (CDFI), there are no blood flow signals in most conditions. Sometimes, "pseudo-color blood flow signals" may occur, which could be an illusion caused by the Doppler effect of ultrasound rather than actual blood flow activity. Due to the organization and fibrous transformation of the clot, the elasticity may

Received 29.07.2025 Accepted 13.09.2025
Med Ultrason
2025, Vol. 27, No 4, 502-503, DOI: 10.11152/mu-4566,
Corresponding author: Xiaoqin Qian
Northern Jiangsu People's Hospital
Yangzhou, 225001, China
E-mail: yz_tyz1030@126.com

be harder than that of the surrounding normal tissue. Unlike neoplastic space-occupying lesions characterized by rich blood vessels, blood clots do not show enhancement under contrast-enhanced ultrasound, which is of great significance for differential diagnosis.

Acknowledgement: This work was funded by Support Technical Project of Northern Jiangsu People's Hospital (FCJS202528).

References

1. Strand E, Meshkin RS, Hoyek S, Miller JB, Patel NA. Non-diabetic Vitreous Hemorrhage: A Review of Management Strategy and Outcomes. Ophthalmic Surg Lasers Imaging Retina 2024;55:660-667.
2. Shaikh N, Srishti R, Khanum A, et al. Vitreous hemorrhage – Causes, diagnosis, and management. Indian J Ophthalmol 2023;71:28-38.

Solitary papule: ultrasonographic findings of cervical chondrocutaneous branchial remnants

Juan Liu*, Zheng-sen Dong*, Ting-yi Wang, Xiao-yi Wang, Pei Hu

** the authors share the first authorship*

Department of Ultrasound, Renmin Hospital, Hubei University of Medicine, Shiyan, China

To the Editor,

A 4-month-old patient was evaluated for a right-sided neck mass that was initially noticed. Physical examination revealed a firm, cartilaginous mass located anterior to the right sternocleidomastoid muscle. The lesion was mobile against the overlying skin, with no associated erythema, ulceration, or discharge (fig 1A). Ultrasonography revealed a superficially protruding, mildly hyperechoic mass in the right neck, with a connecting pedicle to the skin, a central coaxial hypoechoic area (fig 1B), and deep extension tracking centrally along the sternocleidomastoid muscle. No significant internal blood flow was detected on color Doppler imaging (fig 1C). The ultrasonographic features were consistent with cervical chondrocutaneous branchial remnants (CCBRs). Following consultation with pediatric surgery, the mass was surgically excised, histopathological examination confirmed the diagnosis of CCBRs (fig 1D).

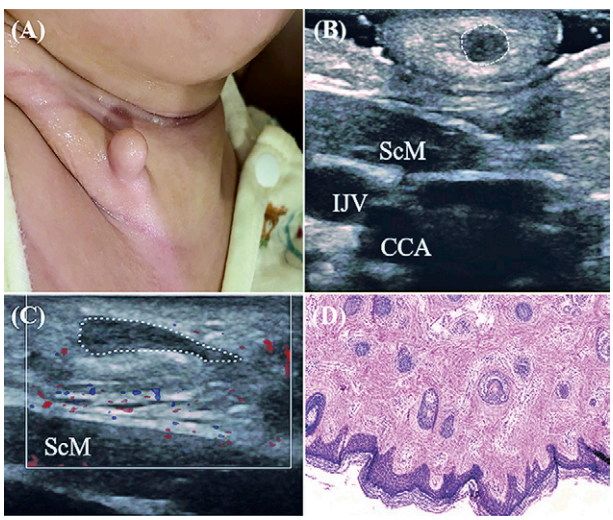

Fig 1. A) Firm, cartilaginous mass anterior to right sternocleidomastoid muscle; B) Transverse view: A 15×6 mm mildly hyperechoic mass with a 3-mm pedicle connecting to the skin and a central coaxial hypoechoic area (white dashed lines). C) Longitudinal view: A 20-mm anechoic tract tracking centrally superficial to the sternocleidomastoid muscle. Color Doppler showed no significant blood flow within the hypoechoic area (white dashed lines). D) Squamous epithelium overlying a mass of adipose tissue, cartilage, and fibrous connective tissue, diagnostic of CCBRs. (H&E, 100X).

Branchial anomalies of the neck, which result from the abnormal development of the branchial apparatus during the 4th to 7th weeks of embryogenesis, account for approximately 20-30% of congenital pediatric head and neck masses [1]. Cervical branchial anomalies encompass a spectrum of congenital conditions, including

Received 15.10.2025 Accepted 08.11.2025
Med Ultrason
2025, Vol. 27, No 4, 503-504, DOI: 10.11152/mu-4567,
Corresponding author: Pei Hu MD
Department of Ultrasound,
Renmin Hospital,
Hubei University of Medicine,
Shiyan 442000, Hubei, China
E-mail: 32737715@qq.com

first and second branchial cleft anomalies, as well as CCBRs. Among these, CCBRs are exceptionally rare, benign congenital neck lesions that most commonly present unilaterally, with bilateral occurrence being exceedingly uncommon [2]. CCBRs typically occur in the middle to lower third of the neck. It is considered to originate from the second or posterior branchial arch and histologically contain cartilage tissue resembling that of the auricle.

This infant presented at birth with a solitary papule or nodule demonstrated cartilaginous consistency without bleeding or discharge. Sonographic evaluation revealed a characteristic band-like anechoic tract extending to the fascia of the sternocleidomastoid muscle, with absent color Doppler flow. These imaging features are consistent with the classic presentation of CCBRs. The differential diagnosis for CCBRs includes cervical lymph nodes, epidermoid cysts, and pilomatricomas. The pathognomonic sonographic finding is a linear, cartilaginous, anechoic structure within the subcutaneous tissue of the neck.

Although most patients with CCBRs are asymptomatic [3]，a minority may develop secondary infections, and rare cases exhibit potential for malignant transformation. Therefore, surgical excision is recommended upon diagnosis.

References

1. LaRiviere CA, Waldhausen JHT. Congenital cervical cysts, sinuses, and fistulae in pediatric surgery. Surgical Clinics 2012;92:583-597.
2. Xu M, Chen L, Gong X, et al. The managements of cervical chondrocutaneous branchial remnants. Lin Chuang Er Bi Yan Hou Tou Jing Wai Ke Za Zhib2023;37:122-126.
3. He Y, Zhu H, Ji H, et al. A case report and literature review of bilateral cervical chondrocutaneous branchial remnants. Case Rep Dermatol Med 2023;2023:8475270.

Are high-frequency and ultra-high-frequency ultrasound useful in pediatric dermatology?

Corrado Tagliati[1], Elisa Molinelli[2], Andrea Sechi[3], Angelo Valerio Marzano[3], Giulio Rizzetto[2], Edoardo De Simoni[2], Matteo Candelora[2], Marco Fogante[4], Claudio Ventura[4], Aritra Kapat[5], Cecilia Lanza[4], Antonio Corvino[6], Giulio Argalia[4], Annamaria Offidani[2], Oriana Simonetti[2]

[1]AST Ancona, Ospedale di Comunità Maria Montessori di Chiaravalle, Chiaravalle, Italy, [2]Department of Clinical and Molecular Sciences, Dermatology Clinic, Polytechnic Marche University, Ancona, Italy, [3]Dermatology Unit, Fondazione IRCCS Ca' Granda Ospedale Maggiore Policlinico, Milan, Italy, [4]Maternal-Child, Senological, Cardiological Radiology and Outpatient Ultrasound, Department of Radiological Sciences, University Hospital of Marche, Ancona, Italy, [5]Department of Pediatric Medicine, Dr BC Roy Post Graduate Institute of Pediatric Sciences, Kankurgachi, Phoolbagan, Kolkata, West Bengal, India, [6]Medical, Movement and Wellbeing Sciences Department, University of Naples "Parthenope", Naples, Italy,

To the Editor,

We would like to express our thoughts about high-frequency and ultra-high-frequency ultrasound in pediatric dermatology.

Why and when this imaging techniques could help a pediatric dermatologist?

Received 26.09.2025 Accepted 08.11.2025
Med Ultrason
2025, Vol. 27, No 4, 504-505, DOI: 10.11152/mu-4568,
Corresponding author: Corrado Tagliati
Via Lambro 5, 60126 Ancona, Italy
E-mail: corrado.tagliati@gmail.com
Phone +39 3662677166

Surely, dermatologic ultrasound can sometimes show clinically undetectable diseases due to its tissue penetration, which is superior to any other dermatologic imaging technique, and the minimum probe frequency required is 15 MHz. However, newer probes available in clinical practice can reach 70 MHz.

Ultrasound is reported to be useful in some dermatologic guidelines, such as melanoma and hidradenitis suppurativa ones. Regarding diagnosis, ultrasound can discriminate between dermatologic and non-dermatologic diseases in presence of a bump, for example excluding a musculoskeletal lesion. Ultrasound can find a piece of broken glass or a fragment of a wooden object and can

help differentiate benign lesions, such as epidermal cyst, trichilemmal cyst, dermatofibroma, pilomatrixoma, lipoma, and neurofibroma. Rarer diseases could also be well evaluated at ultra-high-frequency ultrasonography, such as aplasia cutis congenita and nevus sebaceous of Jadassohn. Obviously, malignant lesions can be suspected at ultrasound.

In regard to disease extension, ultra-high frequency ultrasound Breslow thickness measurement was reported to be highly reliable. Color Doppler ultrasound can show morphea's subclinical activity in areas adjacent to the clinically active lesion, in nonadjacent regions, and demonstrate activity at a clinically inactive lesion site. Ultra-high-frequency ultrasound can precisely evaluate hidradenitis suppurativa disease extension, as very early hair follicles alterations can be easily detected, such as hair follicle increased size and curved shape. Moreover, it is known that fistulous tracts can be perfectly assessed and counted.

Regarding disease scoring, ultrasound morphea activity score (US-MAS) allows to systematically register the cutaneous abnormalities, and sonographic scoring system acne severity classification (SOS-Acne) can be used to objectively grading the disease into mild, moderate and severe. Modified sonographic scoring of hidradenitis suppurativa (mSOS-HS) and ultrasound hidradenitis suppurativa activity scoring (US-HSA) can be used in order to respectively assess disease severity and activity [1].

Pediatric melanoma is a relatively rare disease. However, ultrasound can be very useful for regional metastasis and lymph node involvement detection. Moreover, it can guide fine-needle aspiration.

Related to treatment, ultrasound-assisted intralesional corticosteroid infiltrations for patients with hidradenitis suppurativa non-invasively and cost-effectively enhances the accuracy of triamcinolone injections and improves patients' outcomes. Finally, ultrasound can help evaluate treatment response, such as in infantile hemangioma after oral propranolol therapy or in scabies in order to differentiate between inhabited vs non-inhabited scabiotic burrows after correct treatment with persistent pruritus in cases in which clinical examination or dermoscopy are non-conclusive [2].

Therefore, high-frequency and ultra-high-frequency ultrasound are very useful in pediatric dermatology daily clinical practice, and its use will surely expand in the near future.

References

1. Argalia G, Reginelli A, Molinelli E, et al. High-Frequency and Ultra-High-Frequency Ultrasound in Dermatologic Diseases and Aesthetic Medicine. Medicina (Kaunas) 2025;61:220.
2. Dominguez-Santas M, Roustan-Gullon G, Alfageme-Roldan F. Sonographic findings in scabies. J Ultrasound 2023;26:549-551.

A case of extraconal orbital cavernous venous malformation on sonography

Yiran Wang, Chengfang Yu, Zhe Wang, Yilan Piao

Department of Medical Ultrasound,Yanbian University Hospital, Yanji, Jilin, China

To the Editor,

A 60-year-old male patient presented with a painless mass in the right eye discovered one month prior, without significant visual decline or other discomfort. Examination revealed Vod 1.0, Vos 1.0, 2.5 mm, proptosis of the right eye, cortical and nuclear lens opacities (C2N3), vitreous opacities, and restricted downward movement of the right eye, with normal movement in all other directions and a normal left eye. Bilateral intraocular pressure was palpated as Tn. Ocular ultrasonography showed a well-defined, round, relatively strong echo mass measuring 2.3x2.4 cm located inferolateral to the right globe in the extraconal space, with relatively inhomogeneous internal echoes and enhanced posterior acoustic transmission; Color Doppler Flow Imaging (CDFI) revealed no significant blood flow signal (fig 1a). The ultrasound

Received 29.09.2025 Accepted 08.11.2025
Med Ultrason
2025, Vol. 27, No 4, 505-506, DOI: 10.11152/mu-4569,
Corresponding author: Yilan Piao
Department of Medical Ultrasound,
Yanbian University Hospital
#1327 Juzi St. Yanji 133000, China
E-mail: 1419299989@qq.com

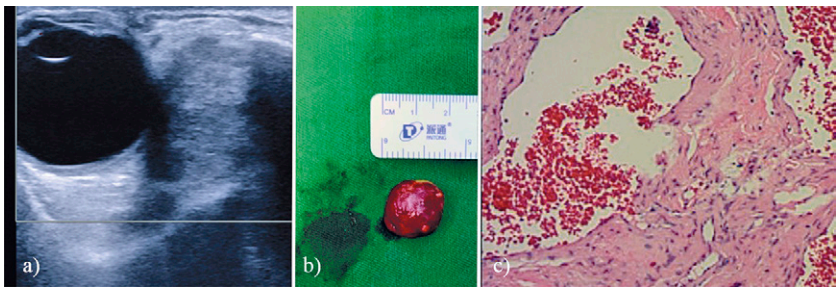

Fig 1. a) Ultrasonography revealed a 2.3x2.4cm, well-defined, round mass inferolateral to the right globe. It demonstrated heterogeneous echotexture with posterior acoustic enhancement and no significant vascularity; b) during the procedure, a dark red, moderately firm mass measuring approximately 2.0 x 2.0 cm was resected; c) postoperative histopathological examination revealed an (orbital) cavernous hemangioma.

findings suggested a solid extraconal orbital mass in the right orbit. The patient underwent general anesthesia for surgical resection of the right orbital mass (fig 1b). Postoperative pathological diagnosis confirmed (orbital) cavernous hemangioma (fig 1c).

Orbital cavernous hemangioma, now more often classified as a venous malformation [1], is the most common benign intraorbital tumor in adults, typically presenting between the ages of 30 and 50 years, with a female predominance. These lesions are most frequently located within the intraconal space, with a minority occurring extraconally. Generally, intraconal lesions are mostly benign, such as cavernous hemangioma, inflammatory pseudotumor, and optic nerve glioma; whereas extraconal lesions have a relatively higher proportion of malignancies, commonly including lymphoma and lacrimal gland epithelial tumors. Specifically, extraconal lymphoma often appears irregular in shape with relatively rich internal blood flow on imaging, while lacrimal gland tumors are typically located in the superolateral orbit involving the lacrimal gland. On ultrasonography, orbital cavernous hemangioma usually presents as a round or oval, well-circumscribed mass with homogeneous internal echoes, mild acoustic attenuation, and some compressibility, with most cases showing insignificant internal blood flow signals. The ultrasonographic features in this case align with the typical presentation of cavernous hemangioma. However, the patient's age, gender, and lesion location (extraconal) are not entirely consistent with the common clinical profile. Therefore, during the diagnostic process, it is crucial to avoid fixed thinking patterns and recognize that this lesion can also occur in the extraconal space. The definitive diagnosis ultimately relies on pathological examination as the gold standard.

Reference

1. Calandriell L, Grimaldi G, Petrone G, et al. Cavernous venous malformation (cavernous hemangioma) of the orbit: Current concepts and a review of the literature. Surv Ophthalmol 2017;62:393-403.

The "silent assassin" of the liver: angiosarcoma with portal hypertension

Xuan Zhang[1], Nina Qu[2], Xiaoli Cao[2]

[1]School of Medical Imaging, Binzhou Medical University, [2]Department of Ultrasound, Yantai Yuhuangding Hospital Affiliated to Qingdao University, Yantai, Shandong, China

Received 31.10.2025 Accepted 19.11.2025
Med Ultrason
2025, Vol. 27, No 4, 506-507, DOI: 10.11152/mu-4570,
Corresponding author: Xiaoli Cao
Department of Ultrasound, Yantai Yuhuangding Hospital Affiliated to Qingdao University, Yantai, Shandong, China
E-mail: xiaolicao969@163.com

To the Editor,

A 73-year-old male was admitted due to recurrent hemoptysis for 20 days. His medical history included hypertension and coronary heart disease. Laboratory tests revealed: RBC 3.93×10^{12}/L, PLT 69×10^{9}/L; coagulation

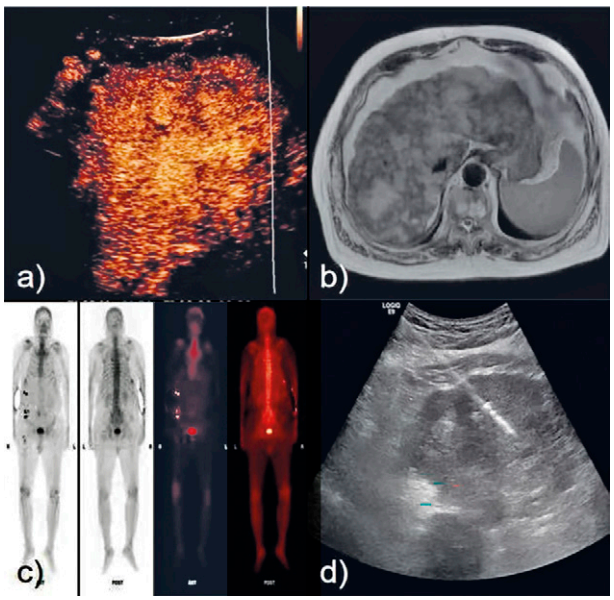

Fig 1. a) Contrast-enhanced ultrasound revealed that the tumor exhibited a diffusely infiltrative growth pattern without distinct margins; b) Contrast-enhanced MRI demonstrated multiple round-like nodules within the liver parenchyma, some of which showed coalescence; c)The Whole-body bone scintigraphy revealed inhomogeneous radiotracer distribution in multiple bilateral ribs, with abnormal foci of increased uptake in the left fifth anterior/posterior rib, right eighth rib, and the L5 vertebral body; d) Ultrasound-guided percutaneous liver biopsy.

profile: PT 16.6s; liver function: TBil 105.9 μmol/L; tumor markers were within normal limits. Ultrasound showed coarse echotexture of the liver parenchyma. Contrast-enhanced ultrasound (CEUS) (fig 1a) demonstrated diffuse heterogeneous enhancement in the left lobe of the liver. Contrast-enhanced MRI (fig 1b) revealed multiple diffuse round-like nodules in the liver parenchyma exhibiting a "fast-in and slow-out" enhancement pattern, suggesting liver cirrhosis with malignancy not excluded. Additionally, splenomegaly, a small amount of ascites, gastric varices, and multiple abnormally enhancing foci in the bones were noted. Whole-body bone scintigraphy (fig 1c) findings were consistent with bone metastases. Ultrasound-guided liver biopsy (fig 1d) confirmed the diagnosis of hepatic angiosarcoma on pathological examination. Immunohistochemical staining was positive for ERG, CD34, CD31, and FLI-1, with strong positive for Ki-67 (70%). The final diagnosis was primary hepatic angiosarcoma (cTxN0M1 Stage IV) with bone metastases. The patient's condition progressed rapidly and treatment was subsequently discontinued.

Primary hepatic angiosarcoma (PHA) is a rare malignant tumor of endothelial origin, predominantly affecting middle-aged and elderly males [1]. This case is notable for its initial presentation of hemoptysis accompanied by cytopenias. Bae et al [2] suggested that infiltrative hepatic angiosarcoma can cause portal hypertension and ascites. The signs of portal hypertension in this patient (splenomegaly, ascites, and gastric varices) were considered to be related to increased intrahepatic microvascular resistance due to tumor infiltration. The prognosis of PHA is extremely poor, with most patients diagnosed at an advanced stage. Surgical resection is the primary modality offering potential long-term survival, while the survival of untreated patients is typically less than 6 months [3]. Therefore, PHA should be suspected in cases of unexplained liver masses accompanied by portal hypertension and coagulopathy.

References

1. Liao X, Lai J, Lin J, et al. Primary and secondary angiosarcomas of the liver: a multi-institutional study of 32 cases. Hum Pathol 2023;137:10-17.
2. Bae G, Dunleavy KA, Hagen C, et al. An Infiltrative Case of Angiosarcoma Causing Portal Hypertension. ACG Case Rep J 2024;11:e01532.
3. Rojas S, Rey Chaves CE, Robledo S, et al. Primary hepatic angiosarcoma: a systematic review. Ann Med Surg (Lond) 2024;86:1601-1605.

Prenatal ultrasound performance of partial placenta membranacea and previa combined with placenta accreta

Juan Wen, Qing-Yun Song

Department of Diagnostic Ultrasound, West China Second University Hospital of Sichuan University, Key Laboratory of Birth Defects and Related Diseases of Women and Children (Sichuan University), Chengdu, China

To the Editor,

The patient was a 29-year-old woman at G2P0 who underwent curettage due to endometrial thickening. A prenatal ultrasound examination at 24 weeks of gestation found the following: the placenta was attached to the anterior, posterior, and left walls of the uterus with a thickness of 2.5 cm. No significant placental parenchymal echoes were seen at the lower segment of the posterior placental wall, and only linear enhancement echoes were noted. Grid-like echo changes were observed at the anterior and lower posterior walls of the uterus and upper cervix (fig 1a). Pulse Doppler showed the venous blood flow spectrum (fig 1b). The ultrasound results were suggestive of placental dysplasia: could the lower placenta be considered placenta membranacea? The lower margin of the placenta covered the internal os, and placenta previa combined with placenta accreta was suspected. MRI examination at 29 weeks of gestation found the following: the placenta did not cover the internal os and increased varicose vascular shadows that could be seen at the retroplacental clear space. Transvaginal ultrasound examination at 36 weeks of gestation showed that there was no sign of placental attachment at 2 cm above the internal os (fig 1c). Transabdominal ultrasound examination at 38 weeks of gestation found that the placenta and cervix images were not clear due to advanced gestational age and blocking by the fetus (fig 1d).

The patient underwent cesarean section at 39 weeks of gestation. During the surgery, partial covering of the internal os by the lower margin of the placenta could be seen. The placenta was widely and densely adhered to the lower segment of the anterior and posterior uterine walls, and some of the placental tissue invaded the lower segment of the uterus and surrounding myometrium of the internal os. Postoperative diagnoses included the following: partial placenta previa, partial placenta membranacea, and placenta accreta.

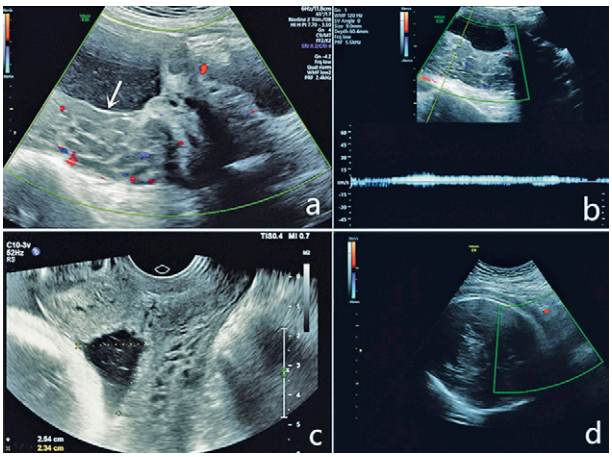

Fig 1. No significant placental parenchymal echoes were seen at the lower segment of the posterior placental wall; only linear enhancement echoes were noted (a, white arrow). Grid-like echo changes were observed at the anterior and lower posterior walls of the uterus and upper cervix (a). Pulse Doppler showed the venous blood flow spectrum (b). Transvaginal ultrasound examination at 36 weeks of gestation showed that there was no sign of placental attachment at 2 cm above the internal os (c). Transabdominal ultrasound examination at 38 weeks of gestation found that the placenta and cervix images were not clear due to advanced gestational age and blocking by the fetus (d).

As there were very few similar cases, it cannot be concluded that linear echoes are a characteristic manifestation of placenta membranacea. Thus, vigilance should be increased when this sign is present, and a careful search for other clues of placenta accreta should be carried out. In this patient, the intramural grid-like echoes were considered to be a manifestation of abnormal intramural vascular dilation caused by placenta accreta. MRI at 29 weeks of gestation also did not identify placenta previa and placenta accreta, showing that missed diagnosis of placenta membranacea and placenta accreta may occur when MRI is used. Furthermore, when gestational age is advanced, these lesions sites (mainly at the posterior wall and cervix) cannot be completely displayed due to blocking by the fetus. Therefore, an early and accurate diagnosis is extremely significant.

Received 09.11.2025 Accepted 12.11.2025
Med Ultrason
2025, Vol. 27, No 4, 508, DOI: 10.11152/mu-4571,
Corresponding author: Qing-Yun Song
Department of Diagnostic Ultrasound,
West China Second University Hospital,
Sichuan University, Chengdu,
Sichuan Province, 610041, China
E-mail : huaxi2chaoshengsqy@163.com